Title
OPTICAL COHERENCE TOMOGRAPHY ANALYSIS OF OUTER RETINAL TUBULATIONS

Journal
Retina, 38(8)

ISSN
0275-004X

Authors
Preti, Rony C
Govetto, Andrea
Filho, Richard Geraldo Aqueta
et al.

Publication Date
2018-08-01

DOI
10.1097/iae.0000000000001810

Peer reviewed

Optical Coherence Tomography Analysis of Outer Retinal Tubulations: Sequential Evolution and Pathophysiological Insights.

Authors: Rony C. Preti[1], Andrea Govetto[2], Richard Geraldo Aqueta Filho[1], Leandro Cabral Zacharias[1], Sergio Gianotti Pimentel[1], Walter Y. Takahashi[1], Mario L.R. Monteiro[1], Jean Pierre Hubschman[2], and David Sarraf[2,3]

1. Division of Ophthalmology, University of São Paulo Medical School, São Paulo, Brazil.
2. Stein Eye Institute, David Geffen School of Medicine at UCLA, Los Angeles, California
3. Greater Los Angeles Veterans Affairs Healthcare Center, Los Angeles, California

None of the authors has a proprietary interest in any aspect of this study.

Corresponding author: Rony Carlos Preti

Address for mailing and reprint requests: Rony Carlos Preti: Av. Ramalho Ortigão, 269 ap. 54, Vila Gumercindo, CEP: 04130-010, São Paulo, Brazil.

mobile phone: 55-11-99991636

Email: preti@usp.br

Key Words:

Outer retinal tubulations, spectral-domain optical coherence tomography, choroidal neovascularization, microcystic macular changes, Müller cells.

Summary statement:

Outer retinal tubulations (ORTs) were divided into forming versus open and closed ORTs. Open ORTs with progressive scrolled edges were significantly associated with microcystic macular abnormalities in the inner nuclear layer (INL) and the outer plexiform layer subsidence sign. The pathophysiology of INL microcystic macular abnormalities may involve Müller cell degeneration.

Abstract

Purpose: To describe the sequential evolution of outer retinal tubulations (ORTs) in patients diagnosed with choroidal neovascularization (CNV) and/or retinal pigment epithelium (RPE) atrophy.

Methods: Retrospective evaluation of spectral-domain optical coherence tomography (SD-OCT) scans of a consecutive cohort of patients with various retinal conditions.

Results: We reviewed the clinical findings of 238 eyes of 119 consecutive patients (54 males and 65 females) with a mean age of 76.2 ± 14.2 years (range: 57-90) and a mean follow up of 3 ± 1.6 years (range 1-7). Over the follow-up period, ORTs were diagnosed in 67 out of 238 eyes (28.1%), 9 of which were imaged with sequential, eye-tracked SD-OCT scans dating from the beginning of ORT formation. The presence of geographic atrophy (GA) and sub-retinal hyperreflective material (SRHM) at baseline were found to be risk factors for ORT development ($p<0.001$ and $p<0.001$, respectively). ORTs were divided into forming versus formed morphologies. The latter was comprised of open and closed ORTs of which the open subtype was the most common. The formation of ORTs was significantly associated with microcystic macular lesions in the inner nuclear layer (INL) and the downward displacement of the outer plexiform layer (OPL), referred to as the OPL subsidence sign ($p<0.001$).

Conclusions: ORT is a frequent OCT finding in eyes with CNV and GA. Open ORTs with progressive scrolled edges and shortened diameter were significantly associated with microcystic macular lesions in the INL and the OPL subsidence sign.

Introduction

Outer retinal tubulations (ORTs) were first described by Curcio et al.[1] in autopsy eyes with neovascular age-related macular degeneration (AMD) and defined as a structural rearrangement of photoreceptors in response to retinal injury. Later, others postulated that ORTs develop in the presence of significant photoreceptor disruption by invagination of remaining cells and scrolling of the external limiting membrane (ELM), leading to the establishment of lateral contact by the outermost photoreceptors.[2-4]

ORTs characteristically develop at the advanced stages of AMD and are associated with poor best corrected visual acuity (BCVA),[5] severe photoreceptor loss and the presence of choroidal neovascularization (CNV) and geographic atrophy (GA).[6] ORTs may also be identified in association with other retinal diseases including eyes with angioid streaks or myopic neovascularization.[7]

With spectral-domain optical coherence tomography (SD-OCT), ORTs appear as round-oval lesions with a hypo-reflective lumen and hyper-reflective borders located in the outer nuclear layer (ONL),[2] while with en-face SD-OCT the morphology of ORTs may resemble a branching network emanating from a fibrovascular scar (Figure 1).[8]

Schaal et al. divided formed ORTs in two main subtypes: open ORTs, in which the hyper-reflective ring is incomplete, and closed ORTs in which the inner segments of the photoreceptors and the ELM completely encircle its lumen. Open and closed ORTs may be preceded by a forming ORT.[6]

Hua et al. proposed that the invagination of the disrupted photoreceptors may lead to the downward displacement of the inner nuclear layer (INL), outer plexiform layer (OPL) and ONL, and named this phenomenon “cynapsis”.[9]

Although morphological characteristics of ORTs have been described in several histopathologic, clinical and cross-sectional reports, the sequential evolution of ORTs remains largely unknown. Recently, Dolz-Marco et al. proposed progressive steps in the formation of ORT focusing mainly on various ELM shapes.[10]

The present study provides further insights into the pathophysiology of ORTs and the sequence of events in ORT development in a consecutive cohort of patients diagnosed with CNV and/or retinal pigment epithelium (RPE) atrophy. Futher, this study explores the significance of characteristic inner and outer retinal changes associated with ORT formation.

Methods

This was a retrospective cohort study that adhered to the principles of the Declaration of Helsinki and was approved by the institutional review board at the University of Sao Paulo.

The inclusion criterion was the presence of unilateral or bilateral CNV, with a minimum follow up of one year. Exclusion criteria were history of retinal detachment, pars plana vitrectomy, complicated phacoemulsification, panretinal photocoagulation, focal macular laser treatment, posterior uveitis and intraocular infections. Medical records and SD-OCT scans were reviewed to ascertain demographic and clinical information of the study population.

SD-OCT images were obtained with the Spectralis SD-OCT with eye-tracking dual-beam technology (Heidelberg EngineeringGmbH, Heidelberg, Germany) and reviewed with the Heidelberg Eye Explorer (version 1.8.6.0) using theHRA/Spectralis Viewing Module (version 5.8.3.0). Each patient was imaged with the 20 x 20 degrees macular volume scan composed by 25 to 49 horizontal B-scans.

BCVA was recorded at each visit in Snellen fraction and was then converted into logarithm of the minimal angle of resolution (logMAR) values for statistical analysis.

The presence of forming ORTs was defined as scrolling of the ELM over a free edge without hypo-reflective lumen (Figure 2, A).

Formed ORTs were defined by SD-OCT as round-oval hyper-reflective lesions with a central hyporeflective lumen, located exclusively in the ONL (Figure 2, B and C) and divided into open and closed ORTs according to Schaal et al.[6] Open ORTs were considered those ORTs with horizontally elongated cross-sections, curving ELM at the ends without complete closure, and nonphotoreceptor cells on the outer aspect (Figure 2, B), while closed ORTs were defined as circular or oval cross-sections with an ELM border and photoreceptors completely encircling its lumen (Figure 2, C).

The presence of the OPL subsidence sign was defined as the focal downward displacement of OPL and INL towards the RPE as illustrated in figure 2, D.[11]

The presence of microcystic macular abnormalities in the INL was defined according to Burggraaff et al.: presence of multiple, hyporeflective cystoid spaces without a cyst wall that are located in the INL and are not confluent with cystoid spaces in other retinal layers, and fail to demonstrate leakage on fluorescein angiography (Figure 2, E).[12]

The presence of RPE atrophy was assessed by a combination of red-free and color fundus photography, fluorescein and indocyanine green angiography, fundus autofluorescence, and the evaluation of SD-OCT scans, and defined as a roughly round or oval area of partial or complete depigmentation of the RPE within the vascular arcades, with thinning of the overlying neurosensory retina.

In eyes with AMD, the diagnosis of geographic atrophy (GA) in color fundus images required the presence within the temporal vascular arcades of at least one patch ≥250 μm of RPE atrophy with clear borders involving the fovea.

Subretinal hyperreflective material (SHRM) was defined as hyperreflective material located

external to the retina and internal to the RPE, as seen with SD-OCT.

Serial tracked SD-OCT B-Scans were carefully reviewed to evaluate the natural history of ORTs.

All the analyses were carried out using the medcalc statistical software version 17.2 (MedCalc Software bvba, available at www.medcalc.org). Descriptive statistics were first calculated for all variables of interest. Decimals were rounded to the nearest tenth. Mean and standard deviation (SD) values were calculated for continuous variables, while frequency and percentage were calculated for categorical variables. Mann-Whitney U test was used to compare quantitative variables between groups, while Chi-Square and McNemar's test were used to compare categorical variables. Univariate and multivariate logistic regression was used to evaluate associations of ORTs with the variables of interest. Differences were reported with 95% confidence intervals. A p value <.05 was considered statistically significant. P values smaller than 0.001 were reported as $p < 0.001$.

Results

We included all consecutive patients, diagnosed with CNV and/or RPE atrophy, who received consultation examination in the division of ophthalmology of the University of São Paulo Medical School in São Paulo, Brazil from January 2010 to Jaunuary 2017. At the end of the review process, we identified 238 eyes from 119 consecutive patients of which 54 (51%) were male and 52 (49%) female, with a mean age of 76.2 ± 14.2 years (range: 57-90) and a mean follow up of 3 ± 1.6 years (range 1-7). Characteristics of the included eyes at baseline and at the end of the follow up period are summarized in table 1.

At baseline, CNV was diagnosed in 135 out of 238 eyes (56.7%) and was unilateral in 103 out of 119 patients (86.5%) and bilateral in the remaining 16 (13.5%). The occurrence of CNV

was due to neovascular AMD in 107 out of 135 eyes (79.2%), angioid streaks in 8 out of 135 eyes (5.9%), central serous chorioretinopathy in 4 out of 135 eyes (3%), high myopia in 9 out of 135 eyes (6.6%) and Vogt-Koyanagy-Harada syndrome in 7 out of 135 eyes (5.3%).

At baseline, all eyes without CNV (103 out of 238, 43.3%) illustrated significant RPE atrophy in the posterior pole, and GA was diagnosed in 16 out of 238 eyes (6.7%).

At presentation, ORTs were diagnosed in 52 out of 238 eyes (21.8%). Mean baseline BCVA in eyes with CNV and ORTs was 0.94 ± 0.52 logMar (range 0.2-2 LogMar, 20/174 Snellen Equivalent), while in eyes with CNV without ORTs it was 0.9 ± 0.49 logMar (range 0.1-2 LogMar, 20/158 Snellen Equivalent), without significant difference (p=0.7).

At baseline, the factors significantly associated with the presence of ORTs in a multivariate logistic regression model were the presence of SHRM (p<0.001), the presence of GA (p<0.001) the presence of microcystic macular abnormalities in the INL (p<0.001) and the OPL subsidence sign (p<0.001).

Differences in central foveal thickness (CFT) were significant between eyes with and without ORTs at baseline. CFT was thickner in eyes with ORTs (492 ± 184 μm, range 203-1144) and thinner in eyes without ORTs (410 ± 209 μm, range 211-1330) with a p- value of 0.001.

At presentation, forming ORTs were present in 13 out of 52 eyes (25%). Formed ORTs were noted in 39 out of 52 eyes (75%), of which 29 (74.4%) were open and 10 (25.6%) were closed.

At presentation, the presence of the OPL subsidence sign was accompanied by ORTs in all cases, and diagnosed in 22 out of 238 eyes (9.2%). In a logistic regression model, the presence of the OPL subsidence sign at baseline was significantly associated with forming and open ORTs (p<0.001) and closed ORTs (p=0.002).

The OPL subsidence sign was always accompanied by microcystic macular lesions in the INL, which were diagnosed in 84 out of 238 eyes (35.3%).

In a multivariate logistic regression model, the presence of microcystic macular changes at baseline was significantly associated with forming and open ORTs ($p=0.003$ and $p<0.001$, respectively) but not with closed ORTs ($p>0.1$).

Over the follow up-period, ORTs developed *de novo* in 15 out of 186 eyes (8.1%), all diagnosed with neovascular AMD. In this subgroup of patients, the sequential evolution of ORTs was documented in 9 eyes (Figure 3) with serial and tracked SD-OCT scans.

In all 9 cases ORT formation started with the scrolling of disrupted ELM and inner segment ellipsoid in proximity of either CNV or RPE atrophy, as illustrated in figure 3, A.

During the follow up period, forming ORTs evolved in all 9 eyes into caverns with hypo-reflective lumen, defined as open ORTs (Figure 3, B).

In all 9 eyes, big open ORTs divided or bifurcated into smaller open ORTs over the follow up period. Before the division, a vertical hyperreflective band of outer retinal tissue appeared at the upper boundary of the open ORTs, marking the region of the split (Figures 3, C and D).

The appearance of microcystic macular abnormalities in the INL associated with the OPL subsidence sign was reported in all 9 eyes in the proximity of open and/or closed ORTs, as illustrated in figures 3 B, C, D, E and F.

In all 9 eyes, small open ORTs evolved into closed ORTs, as illustrated in Figures 3 E and F. In this subgroup of 9 eyes, mean time for ORT formation was 12.7 ± 9 months (range 6-36 months).

Over the follow up period, eyes with CNV were treated with 3.5 ± 2.8 intravitreal bevacizumab injections (range 1-13). Differences between eyes with and without ORTs was not statistically significant ($p=0.3$).

Discussion

Although the morphology and pathophysiology of ORTs have already been described in previous publications,[1-6] to the best of our knowledge the present study is one of the the first[10] to describe the precise sequence of events in the development of ORTs in relationship with characteristic inner and outer retinal changes including microcysts of the INL and OPL subsidence (Figure 4).

The pathohysiology of ORTs is still unclear, but there is evidence that these lesions may represent a response to preserve photoreceptor survival. Progressive damage to photoreceptors may activate the Müller cells and promote the expression of glial fibrillary acidic protein, facilitating ORT formation and bifurcation.[10] This fact may explain the significant association of ORTs with the presence of GA in the present report, suggesting that a dysmorphic or absent RPE facilitates ORTs formation.

In the present study, the sequential evolution of ORTs started with the development of forming ORTs, already described by Schaal et al., which were identified in a zone of ELM and ellipsoid zone disruption (Figure 4, A).[6] Subsequently, forming ORTs evolved into large open ORTs (Figure 4, B), which bifurcated with the formation of multiple smaller open ORTs (Figure 4, C).

Zweifel et al. proposed that intraretinal and subretinal exudation from active CNV may damage the photoreceptor layer, causing focal disruption and presumably triggering ORT bifurcation.[2] However, a bifurcation precursor sign has not yet been described.

In the present study we described with SD-OCT the presence of a hyperreflective vertical line crossing the open ORTs prior to bifurcation (figure 2 C, D). This previously unreported SD-OCT sign may be useful to predict the exact splitting location of these lesions.

Hua et al. described the presence of a novel SD-OCT sign called “cynapsis”, defined as the collapse of the INL, OPL and ONL which separates each ORT. However, the authors did not

provide a pathophysiological explanation of this finding.[9]

Similarly, in the present study we described the downward displacement of the OPL and INL in the proximity of ORTs and speculate that Müller cells may be intricately involved in this process. We refered to this finding as the OPL subsidence sign[11] and it was significantly associated with the presence of ORTs. The OPL subsidence sign should be differentiated from "cynapsis" described by Hua et al as it did not involve the ONL nor was it considered responsible for ORT separation. Although OPL subsidence has been already described as a precursor of drusen-associated atrophy in AMD, this finding has not been previously associated with ORT development.[11]

Müller cells form tight junctions with inner segments of the photoreceptors that comprise the ELM, and the inward scrolling process of the ELM and ellipsoid zone during ORT formation may drag the Müller Cells toward the outer retina, causing the downward displacement of retinal tissue leading to OPL subsidence and the formation of microcystic macular lesions in the INL, a recently described SD-OCT sign also seen in advanced optic neuropathies and tractional disorders.[12-23]

The morphology and location of microcystic macular alterations in optic neuropathies, tractional diosrders (e.g. epiretinal membrane or ERM) and during ORT formation are similar, suggesting a common pathophysiological mechanism. Although discussions on this matter may be speculative, Müller cell degeneration has been proposed as a cause of INL microcystic macular abnormalities.[21] The etiologies of these microcystic lesions may vary, and may include retrograde degeneration of inner retinal layers (as with optic neuropathies) and inner retinal traction (as with vitreomacular interface disorders such as ERM), as proposed by prior studies (Figure 5, A). [21,23] The results of the present study suggest that outward traction associated with OPL subsidence (Figure 5 B and C) may disrupt Müller cells and cause microcystic macular abnormalities in the

INL.

Other mechanisms should be considered, including increased permeability and disruption of the ELM as may occur in advanced AMD. The presence of microcystic macular abnormalities in the INL may represent leakage of fluid from active CNV, but the characteristic small microcystic morphology and the absence of other signs of exudation make this hyphotesis unlikely.

Limitations of this study included the retrospective design and the relatively small number of eyes with long term follow-up while the strength of the study was the long-term follow-up of selected cases with serial, eye tracked SD-OCT scans which allowed the description of the precise sequence of events in ORT formation.

In conclusion, we provided a schematic description of the sequential evolution of ORTs. Forming ORTs evolve into open ORTs, which tend to bifurcate. The bifurcation process is predicted by the appearance of a hyper-reflective line at the site of splitting. The inward scrolling of the free border of open ORTs may drag Müller cells causing OPL subsidence and the appearance of characteristic microcystic macular abnormalities in the INL, which should not be interpreted as sign of CNV activity. Smaller open ORTs tended to evolve into a closed ORT formation.

Further prospective investigations with larger study groups and longer follow up are necessary to confirm our findings on the evolution of ORTs.

References

1. Curcio, CA, Medeiros NE, Millican CL. Photoreceptor loss in age-related macular

degeneration. Invest Ophthalmol Vis Sci 1996; 37: 1236-1249.

2. Zweifel, S. A., M. Engelbert, K. Laud, R., et al. Outer retinal tubulation: a novel optical coherence tomography finding. Arch Ophthalmol 2009; 127: 1596-1602.

3. Litts, KM., Ach T, Hammack KM., et al. Quantitative Analysis of Outer Retinal Tubulation in Age-Related Macular Degeneration from Spectral-Domain Optical Coherence Tomography and Histology. Invest Ophthalmol Vis Sci 2016; 57: 2647-2656.

4. Litts, KM, Messinger JD, Freund KB, et al. Inner Segment Remodeling and Mitochondrial Translocation in Cone Photoreceptors in Age-Related Macular Degeneration with Outer Retinal Tubulation. Invest Ophthalmol Vis Sci 2015; 56: 2243-2253.

5. Lee, JY, Folgar FA, Maguire MG, et al. Outer retinal tubulation in the comparison of age-related macular degeneration treatments trials (CATT). Ophthalmology 2014; 121: 2423-2431.

6. Schaal, KB., Freund KB, Litts KM, et al. Outer retinal tubulation in advanced age-related macular degeneration: Optical Coherence Tomographic Findings Correspond to Histology. Retina 2015; 35: 1339-1350.

7. Giachetti Filho RG, Zacharias LC, Monteiro TV, et al. Prevalence of outer retinal tubulation in eyes with choroidal neovascularization. Int J Retina Vitreous. 2016 Mar 1; 2:6. eCollection 2016.

8. Xuan Y, Zhang Y, Wang M, et al. Multimodal fundus imaging of outer retinal tubulations in choroidal osteoma patients. Retina. 2017 Jan 16. doi: 10.1097/IAE.0000000000001498. [Epub ahead of print]

9. Hua, R., L. Liu, Y. Hu and L. Chen. The occurrence and progression of outer retinal tubulation in Chinese patients after intravitreal injections of ranibizumab. Sci Rep 2015; 5: 7661.

10. Dolz-Marco R, Litts KM, Tan ACS, et al. The Evolution of Outer Retinal Tubulation, a Neurodegeneration and Gliosis Prominent in Macular Diseases. Ophthalmology. 2017 Apr 26. doi: 10.1016/j.ophtha.2017.03.043. [Epub ahead of print].

11. Wu Z, Luu CD, Ayton LN, et al. Optical coherence tomography-defined changes preceding the development of drusen-associated atrophy in age-related macular degeneration. Ophthalmology 2014;121: 2415-22.

12. Burggraaff MC1, Trieu J, de Vries-Knoppert WA, et al. The clinical spectrum of microcystic macular edema. Invest Ophthalmol Vis Sci. 2014; 55:952-961.

13. Pott JW, de Vries-Knoppert WA, Petzold A. The prevalence of microcystic macular changes on optical coherence tomography of the macular region in optic nerve atrophy of non-neuritis origin: a prospective study. Br J Ophthalmol. 2016; 100:216-21.

14. Saidha S, Sotirchos ES, Ibrahim MA, et al. Microcystic macular oedema, thickness of the inner nuclear layer of the retina, and disease characteristics in multiple sclerosis: a retrospective study. Lancet Neurol. 2012 ;11:963-972.

15. Gelfand JM, Nolan R, Schwartz DM, et al. Microcystic macular oedema in multiple sclerosis is associated with disease severity. Brain. 2012; 135:1786-1793.

16. Kisimbi J, Shalchi Z, Mahroo OA, et al. Macular spectral domain optical coherence tomography findings in Tanzanian endemic optic neuropathy. Brain. 2013;136: 3418-3426.

17. Fernandes DB, Raza AS, Nogueira RG, et al. Evaluation of Inner Retinal Layers in Patients with Multiple Sclerosis or Neuromyelitis Optica Using Optical Coherence Tomography. Ophthalmology. 2013;120: 387-394.

18. Kaufhold F, Zimmermann H, Schneider E, et al. Optic neuritis is associated with inner nuclear layer thickening and microcystic macular edema independently of multiple sclerosis. PLoS One. 2013;8(8) :e71145.

19. Wolff B, Basdekidou C, Vasseur V, et al. Retinal inner nuclear layer microcystic changes in optic nerve atrophy: a novel spectral-domain OCT finding. Retina. 2013; 33:2133-2138.

20. Brazerol J, Iliev ME, Höhn R, et al. Retrograde Maculopathy in Patients With Glaucoma. J

Glaucoma. 2017 Feb 6. doi: 10.1097/IJG.0000000000000633. [Epub ahead of print]

21. Abegg M, Dysli M, Wolf S, et al. Microcystic macular edema: retrograde maculopathy caused by optic neuropathy. Ophthalmology. 2014; 121:142-149.

22. Bennett JL, de Seze J, Lana-Peixoto M, et al. Neuromyelitis optica and multiple sclerosis: Seeing differences through optical coherence tomography. Mult Scler. 2015; 21:678-688.

23. Sigler EJ. Microcysts in the inner nuclear layer, a nonspecific SD-OCT sign of cystoid macular edema. Invest Ophthalmol Vis Sci. 2014; 55:3282-3284.

Figure Legends

Figure 1: Spectral-domain optical coherence tomograph en-face imaging of outer retinal tubulations.

In this patient with advanced age-related macular degeneration the morphology of outer retinal tubulations (ORTs) resembles a branching network, with a dendritic pattern. Microcystic macular lesions are well illustrated between the branches of OTRs (white arrows). Note the presence of closed (black arrow) and open ORT (grey arrow) in the 2 registered spectral-domain optical coherence tomography (OCT) B scans and the presence of choroidal neovascularization in the en-face OCT angiogram.

Figure 2: Spectral-domain optical coherence tomography signs of outer retinal tubulations.

A. Forming outer retinal tabulation (ORT). The external limiting membrane (ELM) is scrolling over a free edge (white and black arrows) without a visible hypo-reflective lumen. **B.** Open ORT (white arrow). The hyporeflective lumen is not completely encircled by ELM and ellipsoid (black arrow). **C.** Closed ORTs (white arrows). The hyporeflective lumen is completely encircled by a hyperreflective line corresponding to the ELM (black arrows). **D.** Outer plexiform layer (OPL) subsidence sign (white arrows). The scrolling of the ELM drags the inner nuclear layer (INL) and OPL downwards. Microcystic macular changes in the INL become visible (black arrows). This characteristic sign is also nicely illustrated in figure 2,A. **E.** Presence of microcystic macular lesions in the INL between ORTs (white and black arrows), visible with spectral domain optical coherence tomography as multiple hyporeflective spaces non-confluent with other retinal layers.

Figure 3: Sequential evolution of outer retinal tubulations in an included patient.

A. The formation of outer retinal tubulations (ORTs) begins with the scrolling of disrupted external limiting membrane (ELM) and inner segment ellipsoid (Forming ORTs, white arrow) adjacent to a fibrotic choroidal neovascular membrane. **B.** The scrolling process of the ELM and ellipsoid (black arrow) causes the downward displacement of the outer plexiform layer (OPL) and inner nuclear layer (INL) and the formation of the OPL subsidence sign, which is accompanied by microcystic macular lesions in the INL (white arrow). **C.** A large, open ORT is formed, and a hyperreflective line marking the area of splitting can be seen (white arrow). In the proximity of the open ORT, a closed ORT can be also seen (black arrow). **D.** The open ORT splits in correspondence with the hyperreflective lines (white arrows). **E.** Multiple OPL subsidence signs and corresponding microcystic macular lesions in the INL can be identified (white arrows). Multiple closed ORTs are formed (black arrows). **F.** Partial resolution of the microcystic macular abnormalities in the INL. When the scrolling of ELM and ellipsoid is complete, the outward traction is partially released.

Figure 4. Schematic representation of outer retinal tubulations sequential evolution.

A. The formation of outer retinal tubulations (ORTs) starts in an area of external limiting membrane (ELM) and ellipsoid disruption in the proximity of fibrotic choroidal neovascularization (CNV) or retinal pigment epithelium (RPE) atrophy. The ELM begins to scroll inward at the free edges of the ELM. **B.** A vertical hyperreflective line appears over the resulting open ORT, marking the area of split. **C.** The large open ORT divides into two smaller open ORTs and the margins begin to scroll. The scrolling process causes downward displacement of the outer plexiform layer (OPL) and inner nuclear layer (INL) referred to as the OPL subsidence sign. Microcystic macular lesions develop in association with the OPL subsidence sign. **D.** The open ORTs continue to bifurcate, and

additional microcystic macular abnormalities associated with the OPL susbsidence sign are noted. **E.** Two closed ORTs and one small open ORTs are formed. **F.** The process ends with the formation of three small closed ORTs. The scrolling process ends and the microcystic macular abnormalities in the INL disapprear due to the release of the outward traction.

Figure 5. Formation of microcystic macular lesions in the inner nuclear layer.

A. In a patient with epiretinal membrane, the Müller cells suffer inward traction toward the internal limiting membrane (white arrows) associated with microcystic lesions in the inner nuclear layer (INL). **B.** In a patient with advanced neovascular age-related macular degeneration (AMD) and outer retinal tubulations (ORTs), the Müller cells suffer outward traction toward the retinal pigment epithelium (RPE, white arrows) associated with microcystic lesions in the INL. In both cases, the mechanical forces may disrupt the Müller cells and cause microcystic macular abnormalities in the INL. **C.** The subsidence sign may be encountered in eyes with advanced non-neovascular AMD and geographic atrophy, in which the Müller cells suffer outward traction toward the RPE (white arrow) causing the appearance of microcystic macular lesions in the INL.

Figure 1

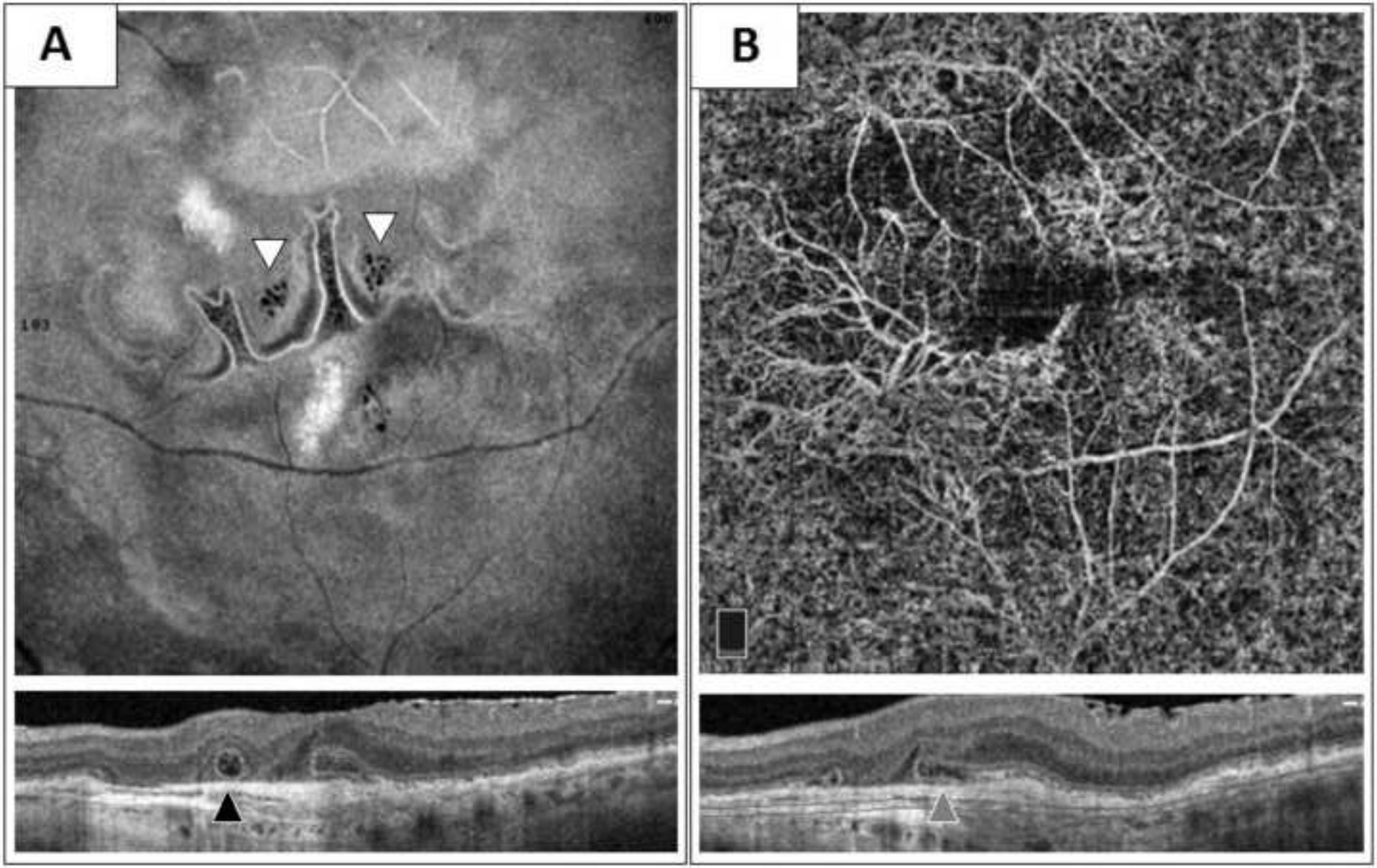

Figure 2

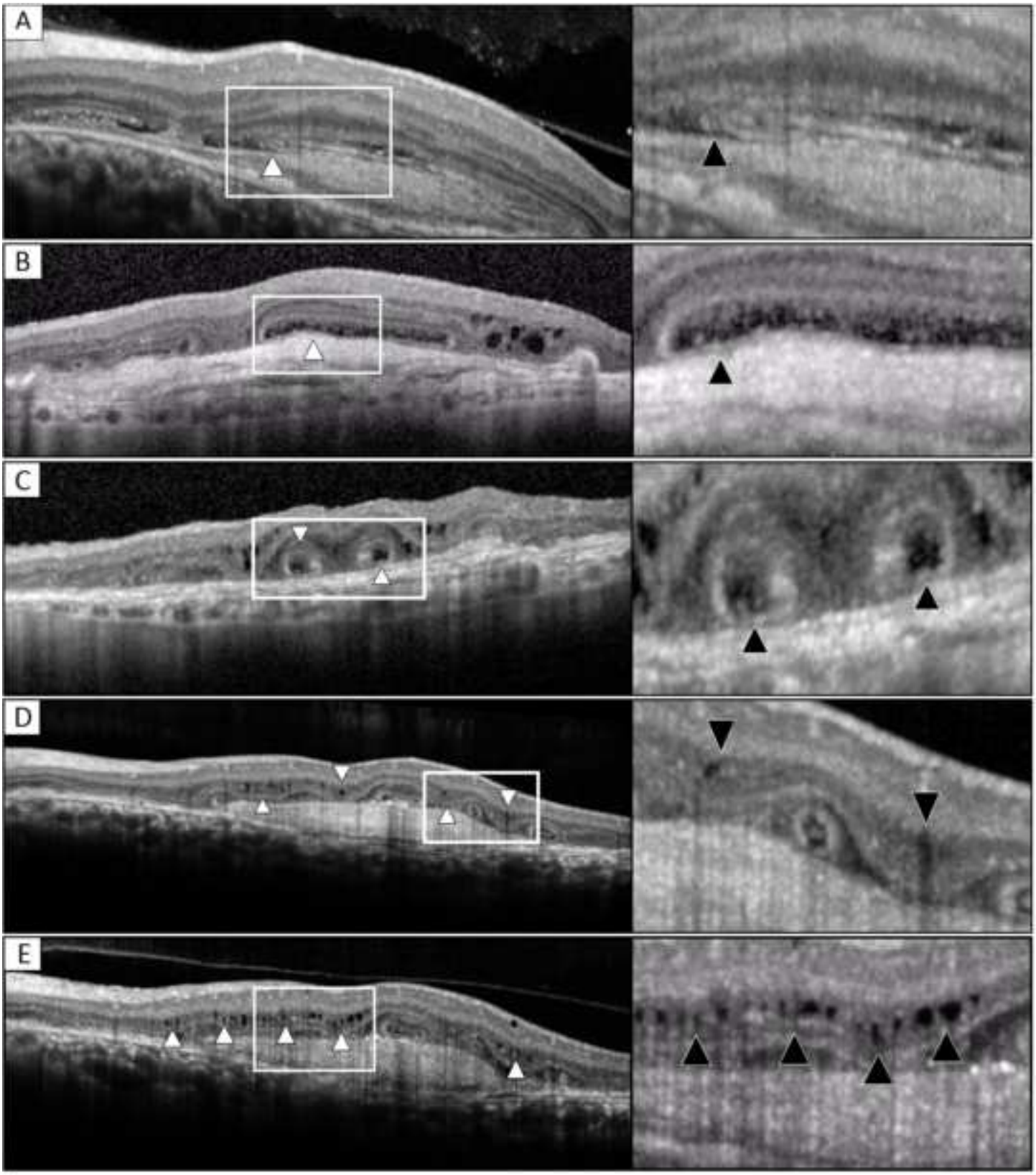

Figure 3

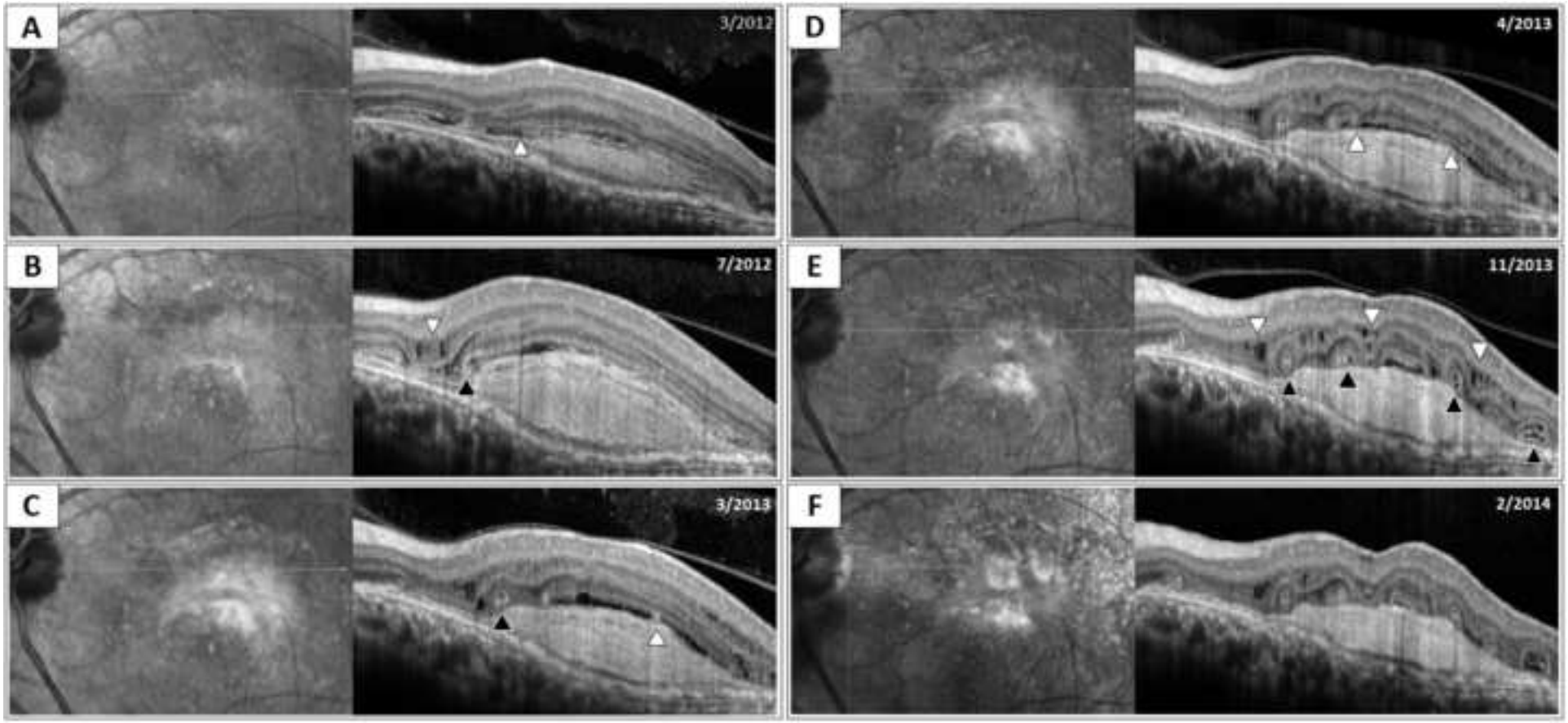

Figure 4

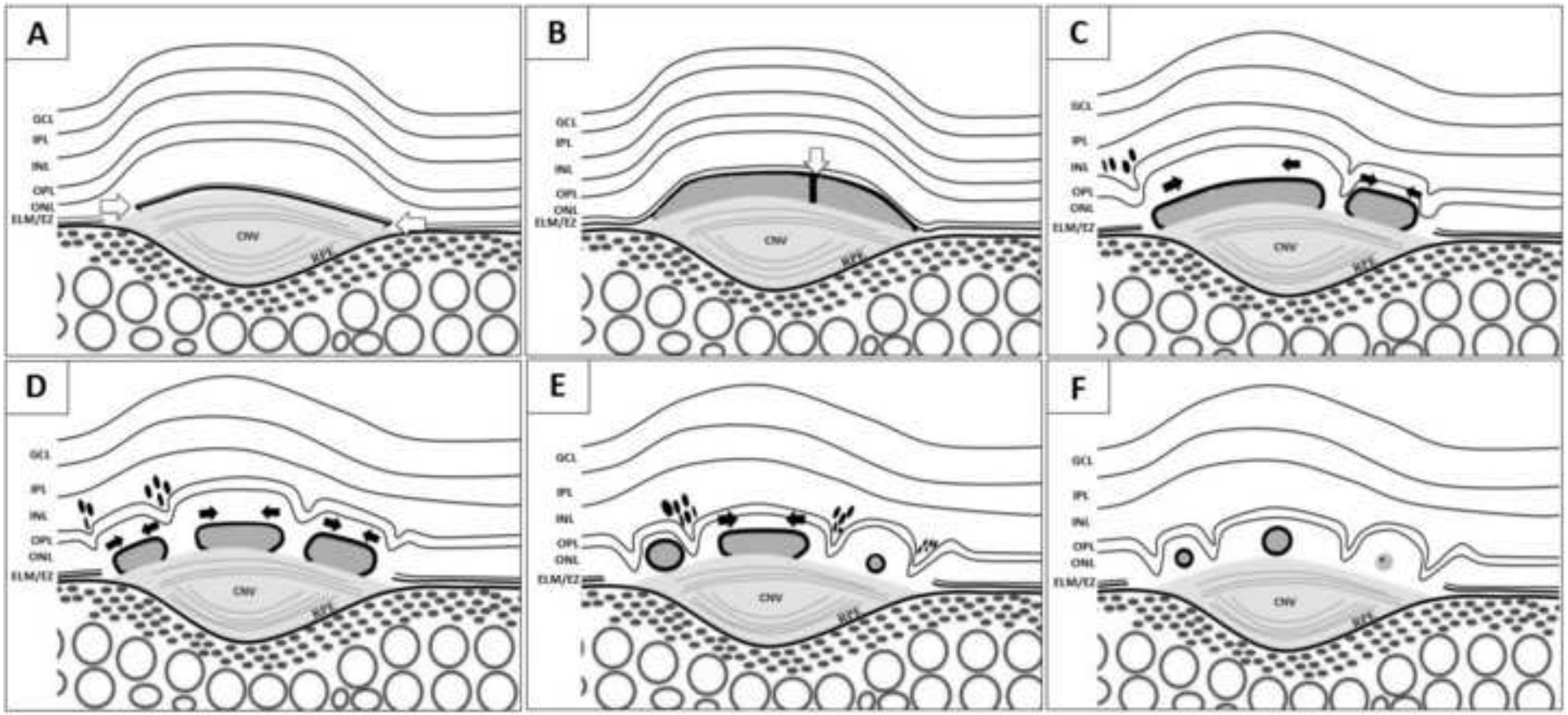

Figure 5

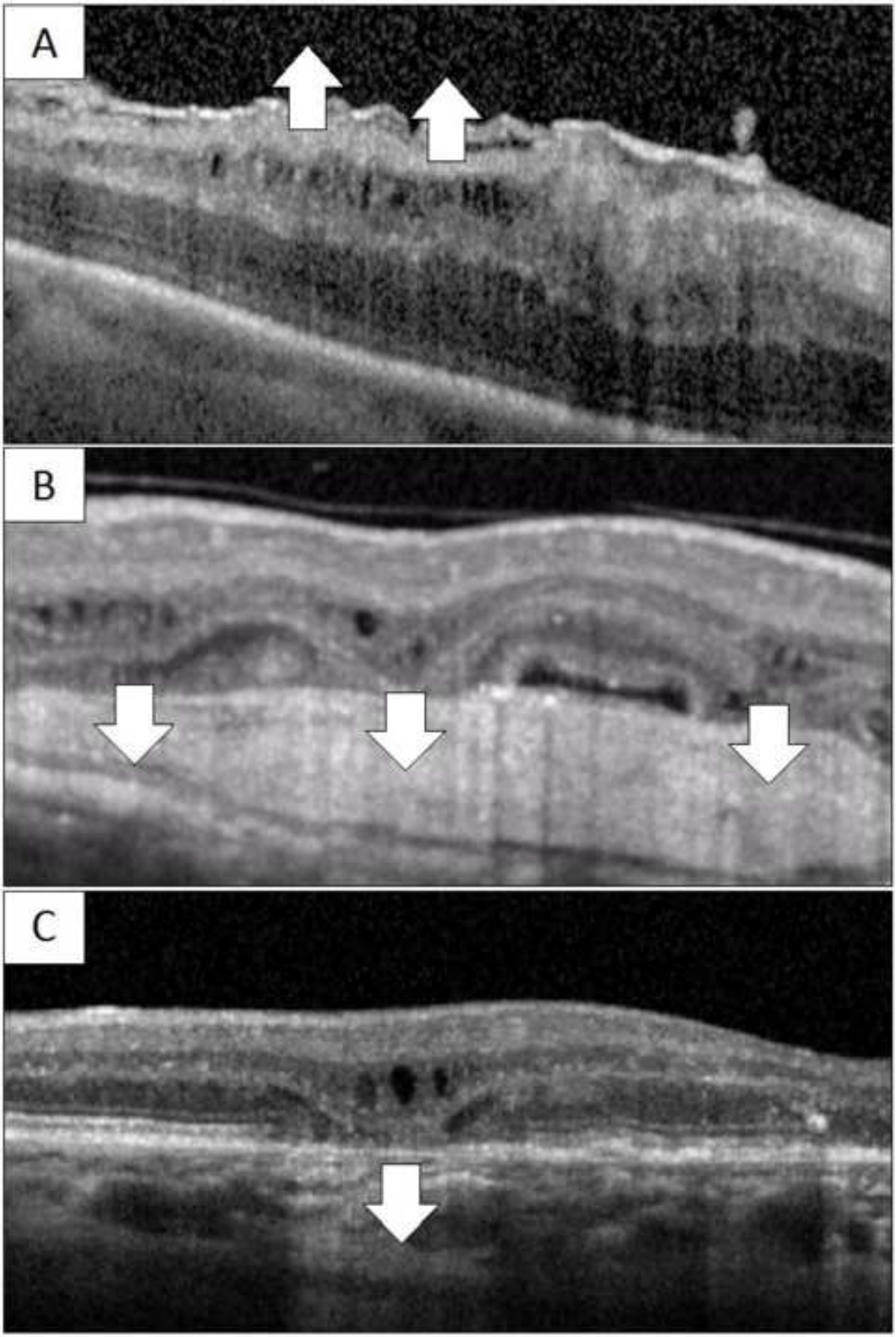

Table 1

Table 1. Characteristics of the included eyes at baseline and at the end of the follow-up period.

	Baseline (n. eyes)	End Follow-Up (n. eyes)	-p value*
ORTs	52	67	0.008
Forming ORTs	13	16	0.647
Open ORTs	29	24	0.383
Closed ORTs	10	20	<0.001
Geographic atrophy	16	34	<0.001
INL microcystic abnormalities	84	86	0.887
SHRM	85	93	0.229

ORTs: Outer retinal tubulations; INL: Inner nuclear layer; SHRM: Subretinal hyperreflective material.

* McNemarʾs test.